# Coordination Networks of $C_{3v}$ and $C_{2v}$ Phenylacetylene Nitriles and Silver(I) Salts: Interplay of Ligand Symmetry and Molecular Dipole Moments in the Solid State†

Wonyoung Choe, Y.-H. Kiang, Zhengtao Xu, and Stephen Lee*

*Department of Chemistry and Chemical Biology, Baker Laboratory, Cornell University, Ithaca, New York 14853-1301*

*Received December 29, 1998. Revised Manuscript Received May 19, 1999*

Five organic ligands of $C_{3v}$ and $C_{2v}$ symmetry, 3,5-bis(4-cyanophenylethynyl)cyanobenzene (**1**), 3,5-bis(4-cyanophenylethynyl)-4-methoxycyanobenzene (**2**), and 4,4′-dicyanobenzophenone (**3**), cyanotris(4-cyanophenyl)methane (**4**), and tris(4-cyanophenyl)methanol (**5**), have been prepared, crystallized with silver(I) salts, and characterized by single-crystal X-ray study. Crystallographic data are as follows: [Ag·**1**·$CF_3SO_3$]·2$C_6H_6$, triclinic, $P\bar{1}$ (no. 2), $a$ = 10.0864(6) Å, $b$ = 13.6029(10) Å, $c$ = 13.8822(12) Å, α = 108.743(6)°, $\beta$ = 95.063(6)°, $\gamma$ = 95.484(5)°, Z = 2; [Ag·**2**·$CF_3SO_3$]·1.75$C_6H_6$, triclinic, $P\bar{1}$ (no. 2), $a$ = 14.6273(14) Å, $b$ = 15.161(2) Å, $c$ = 17.010(2) Å, α = 85.481(7)°, $\beta$ = 65.745(5)°, $\gamma$ = 80.283(9)°, $Z$ = 4; [Ag·**3**·$CF_3SO_3$], triclinic, $P\bar{1}$ (no. 2), $a$ = 8.8148(8) Å, $b$ = 10.5031(6) Å, $c$ = 10.8323(11) Å, α = 81.782(6)°, $\beta$ = 67.448(8)°, $\gamma$ = 66.501(5)°, $Z$ = 2; [Ag·**4**]$BF_4$·1.5$C_6H_6$, monoclinic, $C2/c$ (no. 15), $a$ = 18.0187(4) Å, $b$ = 14.9717(3) Å, $c$ = 23.5469(5) Å, $\beta$ = 105.5641(8)°, $Z$ = 8; [Ag·**5**·$CF_3SO_3$]·2$C_6H_6$, monoclinic, $P2_1/n$ (no. 14), $a$ = 10.230(2) Å, $b$ = 11.839(2) Å, $c$ = 26.071(4) Å, $\beta$ = 90.589(8)°, $Z$ = 4; [Ag·**2**·$CF_3SO_3$]·2$C_6H_6$, triclinic, $P\bar{1}$ (no. 2), $a$ = 14.4951(2) Å, $b$ = 16.5954(1) Å, $c$ = 17.0387(1) Å, α = 84.360(1)°, $\beta$ = 79.728(1)°, $\gamma$ = 73.118(1)°, $Z$ = *4*. The crystal structures are similar to those previously found for the $T_d$ and $D_{3h}$ phenyl nitriles with Ag(I) salts and can be related to the diamond and graphite topologies. However, due to the intrinsic symmetry of $C_{3v}$ and $C_{2v}$ ligands, permanent molecular dipole moments are always present. The stacking sequences found in three graphite-like structures are in an antiparallel fashion so that the net dipole moments of the crystals are zero. Similarly, the diamond-like structure is composed of two interpenetrating diamondoid nets oriented in such a way that the net dipole moment of the two nets combined is zero.

## Introduction

The relationship between molecular structures and their extended structures in the solid state has been a central theme of materials science for the past several years.[1] Recent advances in controlling the extended structures of coordination solids have revealed that networks formed from rigid, symmetric, multitopic ligands[2−4] with directional coordination bonds have structures similar to certain inorganic substances such as graphite, diamond, $ThSi_2$, and PtS. For example, the pseudo-$T_d$ ligand (4,4′,4″,4‴-tetracyanotetraphenylmethane)[2a−b] and the $D_{4h}$ ligands [5,10,15,20-tetra(4-pyridyl)-21*H*,23*H*-porphincopper(II), 5,10,15,20-tetra(4-cyanophenyl)-21*H*,23*H*-porphincopper(II)],[2d] when crystallized with copper(I) salts, form four-connected networks of identical topology to those found in diamond and PtS, respectively. Similarly, the $D_{3h}$ ligand of 1,3,5-tricyanobenzene and silver(I) triflate crystallizes into a graphite-type network while another tritopic $D_{3h}$ ligand, 1,3,5,-tris(4-cyanophenylethynyl)benzene forms a $ThSi_2$-type network under similar condition.[3a−b,5]

* To whom correspondence should be addressed.

† Dedicated to Professor Dr. Peter Böttcher on the occasion of his 60th birthday.

(1) For reviews, see: (a) Desiraju, G. R. *Crystal Engineering: The Design of Organic Solid;* Elsevier: New York, 1989. (b) Robson, R.; Abrahams, B. F.; Batten, S. R.; Gable, R. W.; Hoskins, B. F.; Liu, J. Crystal Engineering of Novel Materials Composed of Infinite Two- and Three-Dimensional Frameworks. In *Supramolecular architecture: synthetic control in thin films*; Bein, T., Ed.; ACS Symposium Series 499; American Chemical Society: Washington, DC, 1992; Chapter 19; p 256. (c) *Comprehensive Supramolecular Chemistry*; Lehn, J.-M., Ed.; Elsevier: New York, 1996; Vols. 6−10. (d) Aakeröy, C. B. *Acta Crystallogr.* **1997**, *B53*, 569. (e) Batten, S. R.; Robson, R. *Angew. Chem., Int. Ed. Engl.* **1998**, *37*, 1461−1494.

(2) A multitopic ligand is one equipped with multiple coordination site and, due to a rigid geometry, is unable to chelate to a metal center. See the examples of Ag(I) or Cu(I) coordination networks based on tetratopic ligands and some other extended structures. (a) Hoskins, B. F.; Robson, R. *J. Am. Chem. Soc.* **1990**, *112*, 1546. (b) Hoskins, B. F.; Robson, R. *J. Am. Chem. Soc.* **1989**, *111*, 5962. (c) Venkataraman, D.; Lee, S.; Moore, J. S.; Zhang, P.; Hirsch, K. A.; Gardner, G. B.; Covey, A. C.; Prentice, C. L. *Chem. Mater.* **1996**, *8*, 2030. (d) Liu, F.-Q.; Tilley, T. D. *Inorg. Chem.* **1997**, *36*, 5090. (e) Abrahams, B. F.; Hoskins, B. F.; Michail, D. M.; Robson, R. *Nature* **1994**, *369*, 727. (f) Fujita, M.; Kwon, Y. J.; Sasaki, O.; Yamaguchi, K.; Ogura, K. *J. Am. Chem. Soc.* **1995**, *117*, 7287−7288. (g) Fujita, M.; Ibukuro, F.; Yamaguchi, K.; Ogura, K. *J. Am. Chem. Soc.* **1995**, *117*, 4175−4176. (h) Yaghi, O. M.; Li, H. *J. Am. Chem. Soc.* **1995**, *117*, 10401−10402. (i) Yaghi, O. M.; Li, G. *Angew. Chem., Int. Ed. Engl.* **1995**, *34*, 207. (j) Li, H.; Davis, C. E.; Groy, T. L.; Kelley, D. G.; Yaghi, O. M. *J. Am. Chem. Soc.* **1998**, *120*, 2186. (k) Fujita, M.; Aoyagi, M.; Ibukuro, F.; Ogura, K.; Yamaguchi, K. *J. Am. Chem. Soc.* **1998**, *120*, 611. (l) Simard, M.; Su, D.; Wuest, J. D. *J. Am. Chem. Soc.* **1991**, *113*, 4696. (m) Wang, X.; Simard, M.; Wuest, J. D. *J. Am. Chem. Soc.* **1994**, *116*, 12119. (n) Su, D.; Wang, X.; Simard, M.; Wuest, J. D. *Supramol. Chem.* **1995**, *6*, 171.

10.1021/cm981153c CCC: $18.00 
Published on Web 06/24/1999

**Chart 1**

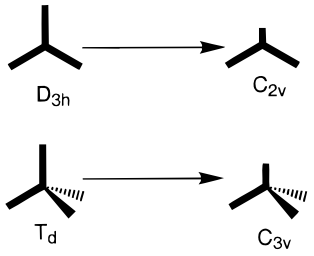


In this paper, we study how changing the symmetry of the ligand affects the extended structure in the solid state. The crystal structures studied here have rigid frameworks and symmetric orientations in their directional bonding similar to the previous $T_d$ and $D_{3h}$ examples. However, the molecular point-group symmetries of the ligands are lowered from $T_d$ to $C_{3v}$ or from $D_{3h}$ to $C_{2v}$. Chart 1 shows the lowering of symmetry from the $T_d$ and $D_{3h}$ symmetry ligands to their $C_{3v}$ and $C_{2v}$ counterparts. One consequence of this symmetry lowering is the introduction of nonzero dipole moments into both the four-coordinate tetratopic and three-coordinate tritopic molecular building units. We report the single-crystal X-ray study of six silver(I) complexes based on these $C_{2v}$ and $C_{3v}$ ligands. These ligands are 3,5-bis(4-cyanophenylethynyl)cyanobenzene (**1**), 3,5-bis(4-cyanophenylethynyl)-4-methoxycyanobenzene (**2**), 4,4′-dicyanobenzophenone (**3**), cyano-tris(4-cyanophenyl)methane (**4**), and tris(4-cyanophenyl)methanol (**5**) (Chart 2).

**Chart 2**

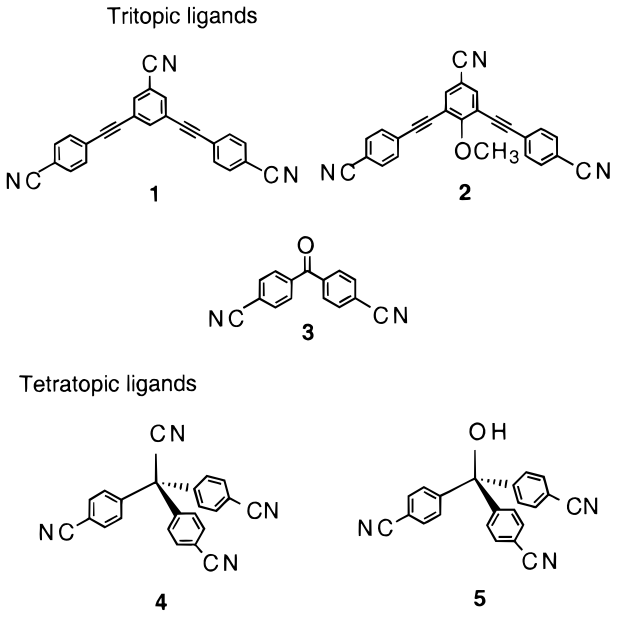


From the six silver(I) complexes studied we deduce three basic principles. First, the individual nets of these structures continue to correspond to the well-known networks such as those found in graphite and diamond. Second, the molecules are oriented in such a way as to make the smallest unit cell of the graphite (or alternatively $AlB_2$) or diamond (or alternatively ZnS) net. Such smallest unit cell nets retain by themselves a nonzero dipole moment but prove to have the densest packing. Third, in each of the six cases studied, a second net is always found which is so oriented that it cancels the first net's total dipole moment.

## Experimental Section

**General Methods.** Unless otherwise indicated, all starting materials were purchased from Aldrich, and used without further purification. Analytical grade solvents were obtained from commercial suppliers (Aldrich, Burdick and Jackson, EM Science, Fisher Scientific, and Mallinckrodt). All atmosphere-sensitive reactions were conducted under nitrogen using a Schlenk vacuum line. Tris(4-cyanophenyl)methanol (**5**) was synthesized according to established procedures.[6] $^1$H NMR and $^{13}$C NMR were performed on Bruker AC-200, AM-300, or A-360. For the crystallization experiments, Teflon-lined screw-caps were used to seal the vials. All crystallizations with the silver(I) salts were achieved by heating and slow cooling in a programmable furnace equipped with a Eurotherm temperature controller. The samples were heated to 90−100 °C, held at that temperature for 90−120 min, and then allowed to cool to room temperature. The heating and cooling profile for each crystallization experiment is described below. No special precautions were employed to exclude oxygen or moisture during crystallization. For X-ray analysis, both mono- and polycrystalline samples were sealed in special glass capillary tubes with ∼1 $\mu$L of the mother liquor to prevent degradation of crystallinity.

(3) See the examples of Ag(I) or Cu(I) coordination networks based on tritopic ligands such as 1,3,5-triazine,[2c] 1,3,5-tricyanobenzne,[3a] 1,3,5-tris(4-ethynylbenzonitrile)benzonitrile,[3a,b] 1,3,5-tris(3-ethynylbenzonitrile)benzonitrile,[3c] 2,4,6-tris(4-pyridyl)-1,3,5-trizine.[3d] (a) Gardner, G. B.; Venkataraman, D.; Moore, J. S.; Lee, S. *Nature*, **1995**, *374*, 792. (b) Reference 2c. (c) D. Venkataraman, D.; Gardner, G.; Lee, S.; Moore, J. S. *J. Am. Chem. Soc.* **1995**, *117*, 11600. (d) Abrahams, B. F.; Batten, S. R.; Hamit, H.; Hoskins, B. F.; Robson, R. *J. Chem. Soc., Chem. Commun.* **1996**, 1690.

(4) See the examples of Ag(I) or Cu(I) coordination networks based on ditopic ligands such as 1,4-pyrazine and its derivatives,[4a−j] 4-cyanopyridine,[4k,l] 1,4-dicyanobenzene,[4m−o] 3,3′-bipyridine,[4p] 4,4′-bipyridine,[4q,r] 4,4′-biphenyldicarbonitrile,[4s,t] and 1,4-bis(4-pyridyl)-butadiyne:[4u,v] (a) Carlucci, L.; Ciani, G.; Proserpio, D. M.; Sironi, A. *J. Chem. Soc., Chem. Commun.* **1996**, 1393. (b) Carlucci, L.; Ciani, G.; Proserpio, D. M.; Sironi, A. *Inorg. Chem.* **1995**, *34*, 5698. (c) Carlucci, L.; Ciani, G.; Proserpio, D. M.; Sironi, A. *Angew. Chem., Int. Ed. Engl.* **1995**, *34*, 1895. (d) Carlucci, L.; Ciani, G.; Proserpio, D. M.; Sironi, A. *J. Am. Chem. Soc.* **1995**, *117*, 4562. (e) Otieno, T.; Rettig, S. J.; Thompson, R. C.; Trotter, J. *Inorg. Chem.* **1993**, *32*, 1607. (f) Otieno, T.; Rettig, S. J.; Thompson, R. C.; Trotter, J. *Can. J. Chem.* **1990**, *68*, 1901. (g) Otieno, T.; Rettig, S. J.; Thompson, R. C.; Trotter, *J. Can. J. Chem.* **1989**, *67*, 1964. (h) MacGillivray, L. R.; Subramanian, S.; Zaworotko, M. J. *J. Chem. Soc., Chem. Commun.* **1994**, *11*, 1325. (i) Kitagawa, S.; Kawata, S.; Kondo, M.; Nozaka, Y.; Munakata, M. *Bull. Chem. Soc. Jpn.* **1993**, *66*, 3387. (j) Kitagawa, S. Munakata, M.; Tanimura, T. *Inorg. Chem.* **1992**, *31*, 1714.L9. (k) Cromer, D. T.; Larson, A. C. *Acta Crystallogr.* **1972**, *B28*, 1052. (l) Carlucci, L.; Ciani, G.; Proserpio, D. M.; Sironi, A. *J. Chem. Soc., Commun.* **1994**, 2755. (m) Reference 2c. (n) Kuroda-Sowa, T.; Horino, T.; Yamamoto, M.; Ohno, Y.; Maekawa, M.; Munakata, M. *Inorg. Chem.* **1997**, *36*, 6382. (o) Venkataraman, D.; Gardner, G. B.; Covey, A. C.; Lee, S.; Moore, J. S. *Acta Crystallogr.* **1996**, *52*, 2416. (p) Lopez, S.; Kahraman, M.; Harmata, M.; Keller, S. W. *Inorg. Chem.* **1997**. *36*, 6138. (q) Lu, J.; Crisci, G.; Niu, T.; Jacobson, A. J. *Inorg. Chem.* **1997**, *36*, 5140. (r) Reference 4l. (s) Hirsch, K. A.; Wilson, R. W.; Moore, J. S. *Chem. Eur. J.* **1997**, *3*, 765. (t) Hirsch, K. A.; Venkataraman, D.; Wilson, S. R.; Moore, J. S.; Lee, S. *J. Chem. Soc., Chem. Commun.* **1995**, 2199. (u) Blake, A. J.; Champness, N. R.; Khlobystov, A.; Li, W.-S.; Schroder, M.; Lemenovskii, D. A. *J. Chem. Soc., Chem. Commun.* **1997**, 2027. (v) Abrahams, B. F.; Hardie, M. J.; Hoskins, B. F.; Robson, R.; Sutherland, E. E. *J. Chem. Soc., Chem. Commun.* **1994**, 1049.

(5) For other frameworks related to inorganic structures such as rutile[5a] and α-Po[5b−f] structures, see: (a) Batten, S. R.; Hoskin, B. F.; Robson, R. *J. Chem. Soc., Chem. Commun.* **1991**, 445. (b) Abrahams, S. C.; Bernstein, J. L.; Liminga, R.; Eisenmann, E. T.; *J. Chem. Phys.* **1980**, *73*, 4585. (c) Hoskins, B. F.; Robson, R.; Scarlett, N. V. Y. *J. Chem. Soc., Chem. Commun.* **1994**, 2025. (d) Soma, T.; Yuge, H.; Iwamoto, T. *Angew. Chem., Int. Ed. Engl.* **1994**, *33*, 1665. (e) Reference 4c. (f) Hoskins, B. F.; Robson, R.; Slizys, D. A. *Angew. Chem., Int. Ed. Engl.* **1997**, *36*, 2752.

(6) Duennebacke, D.; Neumann, W. P.; Penenory, A.; Stewen, U. *Chem. Ber.* **1989**, *122*, 533.

**Table 1. Crystallographic Data for Complexes 6−11[a]**

| complex | 6 | 7 | 8 | 9 | 10 | 11 |
|---|---|---|---|---|---|---|
| chemical formula | $C_{38}H_{23}N_3F_3O_3SAg$ | $C_{37.5}H_{23.5}N_3F_3O_4SAg$ | $C_{16}H_8N_2F_3O_4SAg$ | $C_{32}H_{21}N_4BF_4Ag$ | $C_{35}H_{25}N_3F_3O_4SAg$ | $C_{39}H_{25}N_3F_3O_4SAg$ |
| formula weight | 766.52 | 777.02 | 489.17 | 656.21 | 748.51 | 796.55 |
| crystal system | triclinic | triclinic | triclinic | monoclinic | monoclinic | triclinic |
| space group | $P\bar{1}$ | $P\bar{1}$ | $P\bar{1}$ | $C2/c$ | $P2_1/n$ | $P\bar{1}$ |
| crystal color | colorless | colorless | colorless | colorless | colorless | colorless |
| $a$ (Å) | 10.0864(6) | 14.6273(14) | 8.8148(8) | 18.0187(4) | 10.230(2) | 14.4951(2) |
| $b$ (Å) | 13.6029(10) | 15.161(2) | 10.5031(6) | 14.9717(3) | 11.839(2) | 16.5954(1) |
| $c$ (Å) | 13.8822(12) | 17.010(2) | 10.8323(11) | 23.5469(5) | 26.071(4) | 17.0387(1) |
| α (deg) | 108.743(6) | 85.481(7) | 81.782(6) | 90.00 | 90.00 | 84.360(1) |
| $\beta$ (deg) | 95.063(6) | 65.745(5) | 67.448(8) | 105.5641(8) | 90.589(8) | 79.728(1) |
| $\gamma$ (deg) | 95.484(5) | 80.283(9) | 66.501(5) | 90.00 | 90.00 | 73.118(1) |
| $V$ (Å$^3$) | 1781.1(3) | 3389.5(8) | 849.3(2) | 6119.3(4) | 3157.5(11) | 3854.49(5) |
| $Z$ | 2 | 4 | 2 | 8 | 4 | 4 |
| $\rho_{calc}$ (cm$^{-1}$) | 1.429 | 1.523 | 1.913 | 1.425 | 1.575 | 1.373 |
| $\mu$ (cm$^{-1}$) | 6.80 | 7.18 | 13.67 | 7.10 | 7.67 | 6.33 |
| unweighted agreement factor (R1) | 0.0849 (all data) 0.0575 ($F_o > 4\sigma$) | 0.0849 (all data) 0.0553 ($F_o > 4\sigma$) | 0.0349 (all data) 0.0294 ($F_o > 4\sigma$) | 0.1089 (all data) 0.0660 ($F_o > 4\sigma$) | 0.1659 (all data) 0.0521 ($F_o > 4\sigma$) | 0.1704(all data) 0.1117($F_o > 2\sigma$) |
| weighted agreement factor ($wR2$) | 0.0957 (all data) 0.0935 ($F_o > 4\sigma$) | 0.0998 (all data) 0.0957 ($F_o > 4\sigma$) | 0.0784 (all data) 0.0770 ($F_o > 4\sigma$) | 0.0997 (all data) 0.0930 ($F_o > 4\sigma$) | 0.0676 (all data) 0.0556 ($F_o > 4\sigma$) | 0.3198(all data) 0.2751($F_o > 2\sigma$) |

X-ray data were collected on a Syntex $P2_1$ system or a Siemens Smart diffractometer equipped with a CCD area detector using Mo Kα radiation. Diffraction data were collected at ambient temperatures unless otherwise indicated. All structure solutions were obtained by direct method and refined using full-matrix least squares on all reflections, on the basis of $F_o^2$, with Shelxl 93[7] or Shelx 97. Only the atoms located in the silver(I) salts were refined anisotropically. The ligand hydrogen atoms were included in the last stage of refinement at their geometrically constrained positions. A summary of crystallographic data for the complexes is listed in Table 1. Tables of bond distances, bond angles, anisotropic thermal factors, and observed and calculated structure factors appear in the Supporting Information.

Powder X-ray diffraction data were recorded on an Enraf-Nonius Gunier Camera at 13 mA, 40 kV or an Inel X-ray Diffractometer with a CPS-120 detector at 30 mA, 35 kV for Cu $K\alpha_1$; $\lambda = 1.5406$ Å. Reflections were calibrated with an external standard silver(I) bohemate salt and silicon powder. Lattice constants were fitted and powder data were indexed with a least-squares method.

**3,5-Bis(4-cyanophenylethynyl)cyanobenzene (1).** A heavy-walled Schlenk tube equipped with a Teflon screw-cap was charged with 3,5-dibromobenzonitrile (1.04 g, 4.0 mmol),[8] 4-ethnylbenzonitrile,[9] (1.12 g, 8.8 mmol), copper(I) iodide (33.5 mg, 0.18 mmol), triphenylphosphine (231 mg, 0.88 mmol), bis-(dibenzylideneacetone)palladium(0) (101 mg, 0.18 mmol), and triethylamine(35 mL). The tube was degassed, back-filled with nitrogen three times, sealed with the Teflon screw-cap, and stirred at 70 °C for 12 h in an oil bath. The reaction mixture was allowed to cool to room temperature and filtered through a fritted glass funnel. The filtrate was evaporated to dryness under reduced pressure on a rotary evaporator. Column chromatography on silica gel (2/1, dichloromethane/hexane (v:v)) afforded **1** as a white solid (0.40 g, 28% yield): $^1$H NMR (300 MHz, $CDCl_3$) $\delta$ 7.62−7.71 (m, 8H), 7.81 (d, $J = 1.5$ Hz, 2H), 7.92 (t, $J = 1.5$ Hz, 1H); $^{13}$C NMR (300 MHz, $CDCl_3$) $\delta$ 90.0, 90.8, 112.8, 114.0, 117.0, 118.2, 124.7, 126.8, 132.3, 132.4, 134.8, 138.4; HRMS (EI, 70 eV) calcd 353.0951, found 353.0943.

**3,5-Bis(4-cyanophenylethynyl)-4-methoxycyanobenzene (2).** A heavy-walled Schlenk tube equipped with a Teflon screw-cap was charged with 3,5-dibromo-4-methoxybenzonitrile (487 mg, 1.67 mmol, Lancaster), 4-ethnylbenzonitrile[9] (420 mg, 3.3 mmol), copper(I) iodide (12.6 mg, 0.066 mmol), triphenylphosphine (86.6 mg, 0.33 mmol), bis(dibenzylideneacetone)palladium(0) (38.3 mg, 0.067 mmol), and triethylamine (16 mL). The tube was degassed, back-filled with nitrogen three times, sealed with the Teflon screw-cap, and stirred at 70 °C for 16 h in an oil bath. The reaction mixture was then allowed to cool to room temperature and filtered through a fritted glass funnel. The filtrate was evaporated to dryness under reduced pressure on a rotary evaporator. Column chromatography (2/1, dichloromethane/hexane, (v:v)) on silica gel afforded **2** as a white solid (0.42 g, 66% yield): $^1$H NMR (400 MHz, $CDCl_3$) $\delta$ 7.53−7.61 (m, 8H), 7.70 (s, 2H), 4.19 (s, 3H); $^{13}$C NMR (400 MHz, $CDCl_3$) $\delta$ 61.9, 87.2, 94.4, 107.9, 112.8, 117.1, 117.7, 118.4, 127.2, 132.35, 132.44, 137.8, 164.9; HRMS (EI, 70 eV) calcd 383.1056, found 383.1052.

**4,4′-Dicyanobenzophenone (3).** A three-neck flask equipped with a magnetic stirrer and thermometer was charged with 4-bromobenzonitrile (2.26 g, 12.4 mmol). The flask was immediately capped with septa, then degassed, and back-filled with nitrogen three times. Anhydrous *n*-hexane (15 mL) and anhydrous tetrahydrofuran (THF) (50 mL) were added into this flask via syringe. This mixture was cooled to −98 °C in a cold bath (methanol/liquid nitrogen). While maintaining the temperature below −92 °C, *n*-BuLi (12.4 mmol) in hexane was added via syringe with vigorous stirring. Subsequently a solution of methyl 4-cyanobenzoate (1.0 g, 6.2 mmol) in THF (5 mL) was added via syringe over a 30-min period. The reaction mixture was allowed to warm to room temperature, washed with water, dried over $Na_2SO_4$, and filtered through a fritted glass funnel. The filtrate was evaporated to dryness under reduced pressure on a rotary evaporator. Column chromatography (1/4, ethyl acetate/hexane, (v:v)) afforded **3** as a white solid (0.61 g, 42% yield): $^1$H NMR (400 MHz, $CDCl_3$) $\delta$ 7.82−7.89 (m, 8H); HRMS (EI, 70 eV) calcd 232.0635, found 232.0639

**Cyanotris(4-cyanophenyl)methane (4).** Tris(4-cyanophenyl)methanol[6] (0.3 g, 0.9 mmol) was dissolved in anhydrous benzene (1 mL) and pyridine (0.2 mL), followed by the addition of $SOCl_2$ (2 mL). The system was then sealed with a drying tube. After refluxing at 90−100 °C for 2h in an oil bath, the reaction mixture was allowed to cool to room temperature and evaporated to dryness on a rotary evaporator and then on a vacuum line. Without further purification, the yellowish intermediate product thus obtained was dissolved in DMF (5 mL), followed by addition of NaCN powder (0.2 g, 0.4 mmol), stirred at room temperature overnight, and finally heated to 50 °C for 3 h. The reaction mixture was poured into ice−water,

(7) Sheldrick, G. M. *A Crystal Structure Solution Program*; Institute für Anorg. Chemie: Göttingen, Germany, 1993.

(8) For the procedure from bromobenzoic acid to bromobenzonitrile, see: Doyle, T. J.; Haseltine, J. *J. Heterocycl. Chem.* **1994**, *31*, 1417.

(9) For the synthetic procedures of 4-ethenylbenzonitrile, see: (a) Hirsch, K. A.; Wilson, R. W.; Moore, J. S. *Inorg. Chem.* **1997**, *36*, 2960. Also, for examples of the preparation of phenylacetylenes via palladium-catalyzed cross coupling reactions, see: (b) Zhang, J.; Pesak, D. J.; Ludwick, J. L.; Moore, J. S. *J. Am. Chem. Soc.* **1994**, *116*, 4227. (c) Xu, Z.; Moore, J. S. *Angew. Chem., Int. Ed. Engl.* **1993**, *32*, 1354.

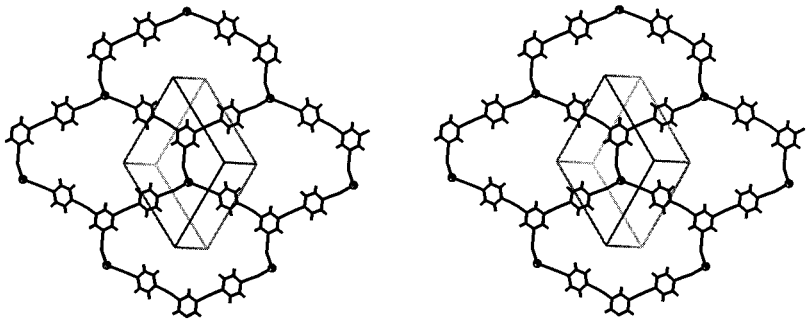

**Figure 1.** Stereoview of the graphitic sheet structure in complex **6**. Solvent molecules as well as triflate ions incorporated in this structure are omitted for clarity. Large circles correspond to Ag sites.

and extracted with dichloromethane (3 × 10 mL). The combined extracts were washed with water three times, dried with $Na_2SO_4$, filtered, and evaporated to dryness on a rotary evaporator. Column chromatography (dichloromethane) afforded **4** as a white solid (0.23 g, 74% yield): $^1$H NMR (200 MHz, $CDCl_3$) $\delta$ 7.26−7.33 (m, 6H), 7.68−7.73 (m, 6H); $^{13}$C NMR (300 MHz, $CDCl_3$) $\delta$ 167.8, 133.2, 132.5, 131.0, 129.5, 128.9, 68.3; HRMS (EI, 70 eV) calcd 344.1061, found 344.1064; MS (EI, 70 eV) 344 ($M^+$, 100), 317 (5.6), 242 (72), 215 (70), 149 (33); IR 2960, 2931, 2874, 2860, 2232, 1728, 1605, 1503 $cm^{-1}$.

**[Ag·1·$CF_3SO_3$]·2$C_6H_6$ (6).** A solution of silver(I) triflate (6.9 mg, 0.27 mmol) in benzene (3.5 mL) was added to a solution of **1** (9.5 mg, 0.27 mmol) in benzene (3.5 mL) in a clean flask equipped with a Teflon-lined screw-cap. A white precipitate formed immediately. The sealed vial was heated to 95 °C at 30 °C/h, held at this temperature for 100 min, and then cooled to room temperature at 0.6 °C/h. Colorless needles formed at the bottom of the vial. Solution $^1$H NMR (300 MHz, DMSO) found the molar ratio of ligand **1** to benzene in the crystal to be 1:2. X-ray powder diffraction of the bulk product showed only one crystal phase which corresponds to the single-crystal structure.

**[Ag·2·$CF_3SO_3$]·1.75$C_6H_6$ (7) and [Ag·2·$CF_3SO_3$]·2$C_6H_6$ (11).** A solution of silver(I) triflate (7.8 mg, 0.3 mmol) in benzene (5 mL) was added to a solution of **2** (11 mg, 0.3 mmol) in benzene (5 mL) in a clean flask equipped with a Teflon-lined screw-cap. A white precipitate formed immediately. The sealed vial was heated to 95 °C, held at this temperature for 90 min, and then cooled to room temperature at 1.2 °C/h. Colorless needles formed at the bottom of the vial. Solution $^1$H NMR (300 MHz, DMSO) found the molar ratio of ligand **2** to benzene in the crystal to be 1:1.75 to 2. X-ray powder diffraction showed only one single-crystal phase which corresponds to single-crystal structure **11**.

**[Ag·3·$CF_3SO_3$] (8).** A solution of silver(I) triflate (2.6 mg, 0.01 mmol) in benzene (2 mL) was added to a solution of **3** (2.3 mg, 0.01 mmol) in benzene in a clean flask equipped with a Teflon-lined screw-cap. A white precipitate formed immediately. The sealed vial was heated to 100 °C, held at this temperature for 90 min, and then cooled to room temperature at 1.2 °C/h. Colorless needlelike crystals suitable for X-ray data collection formed at the bottom of the vial. Solution $^1$H NMR (300 MHz, DMSO) found no benzene molecules included in the crystal. X-ray powder diffraction of the bulk product showed only one crystal phase which corresponds to the single-crystal structure.

**[Ag·4·]$BF_4$·1.5$C_6H_6$ (9).** A solution of silver(I) triflate (2.6 mg, 0.1 mmol) in benzene (2 mL)was added to solution of **4** (3.4 mg, 0.1 mmol) in benzene (2 mL) in a clean flask equipped with a Teflon-lined screw-cap. The sealed vial was heated to 95 °C, held at this temperature for 120 min, and then cooled to room temperature at 1.2 °C/h. Colorless, needlelike crystals suitable for X-ray data collection resulted at the bottom of the vial.

**[Ag·5·$CF_3SO_3$]·2$C_6H_6$ (10).** A solution of silver(I) triflate (2.6 mg, 0.01 mmol) in benzene (2 mL) was added to another benzene solution of **5** (3.4 mg, 0.01 mmol) in a clean flask equipped with a Teflon-lined screw-cap. The sealed vial was heated to 100 °C, held at this temperature for 100 min, and then cooled to room temperature at 1.2 °C/h. Colorless needles suitable for X-ray data collection resulted. Solution $^1$H NMR (300 MHz, DMSO) found the molar ratio of ligand **5** to benzene in the crystal to be 1:2. X-ray powder diffraction of the bulk product showed only one crystal phase which corresponds to the single-crystal structure.

## Results

**Graphitic Sheet Structure of [Ag·1·$CF_3SO_3$]·2$C_6H_6$ (6).** The crystal structure of **6** is illustrated in Figure 1. The silver atoms are in a trigonal-pyramidal geometry and are bonded to three ligand nitrogen atoms at Ag−N distances of 2.206(6), 2.217(6), and 2.306(5) Å. The triflate counterions occupy the axial positions of the trigonal pyramids with a Ag−O distance of 2.447-(6) Å. Each silver atom bonds to three tritopic ligands and each tritopic ligand **1** bonds to three silver atoms. This alternation between the silver atoms and the ligands leads to a planar, honeycomb-type sheet structure similar to that found in graphite. The average plane-to-plane distance is 3.37 Å. The observed staggered arrangement of benzene rings from one sheet to the next is frequently found in organic crystals and is often attributed to the $\pi-\pi$ interaction.[10] The solvent benzene molecules, which participate in $\pi-\pi$ interaction, reside on the graphite-type sheets. Though the structure has channels running along [$\bar{1}$ 1 1] axis, the hexagon-shaped voids are filled with solvent molecules as well as triflate counterions.

**Graphitic Sheet Structures of [Ag·2·$CF_3SO_3$]·1.75$C_6H_6$ (7) and [Ag·2·$CF_3SO_3$]·2$C_6H_6$ (11).** Figure 2 illustrates the crystal structure of **7** and **11**. As in the case of complex **6**, the overall structures are two-dimensional honeycomb-type nets with average plane-to-plane distances of 3.51 and 3.53 Å, respectively. There are two crystallographically distinct silver sites for both structures. Silver atoms reside in a trigonal-pyramidal geometry as complex **6**, and bond to three ligand nitrogen atoms and one triflate oxygen atom. In complex **7**, one triflate counterion bonds simultaneously to both types of silver while in complex **11** each triflate is bonded to only a single silver atom. Bridging triflate ions are well-known in silver(I) triflate−organic complexes.[11c] The honeycomb-shaped channels are filled with solvent molecules and triflate counterions.

**Graphitic Sheet Structure of [Ag·3·$CF_3SO_3$] (8).** The crystal structure of **8** is illustrated in Figure 3. The

(10) Shetty, A. S.; Zhang, J.; Moore, J. S. *J. Am. Chem. Soc.* **1996**, *118*, 1019 and references therein.

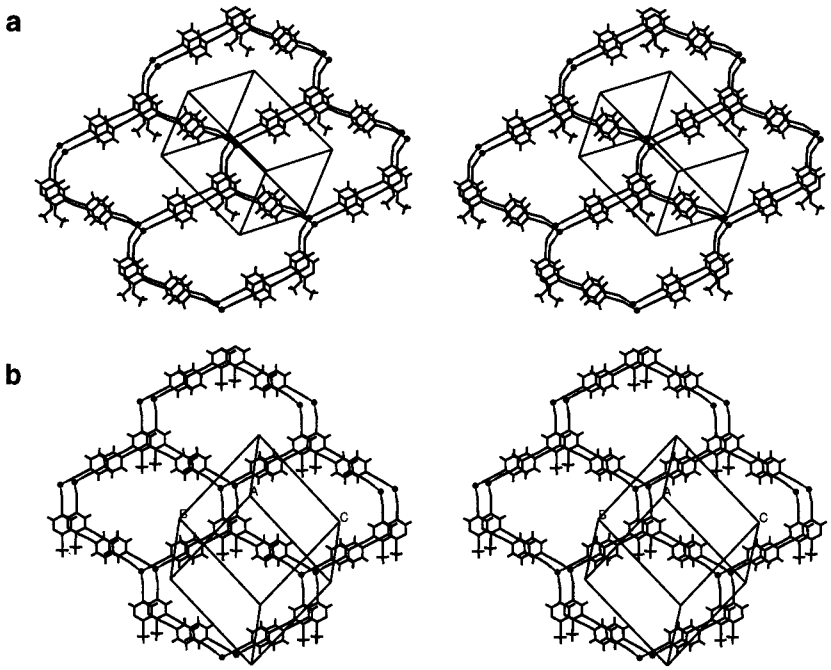


**Figure 2.** Stereoviews of the graphitic sheet structures in (a) complex **7** and (b) complex **11**. Solvent molecules as well as triflate ions incorporated in these structures are omitted for clarity. Large circles correspond to Ag sites.

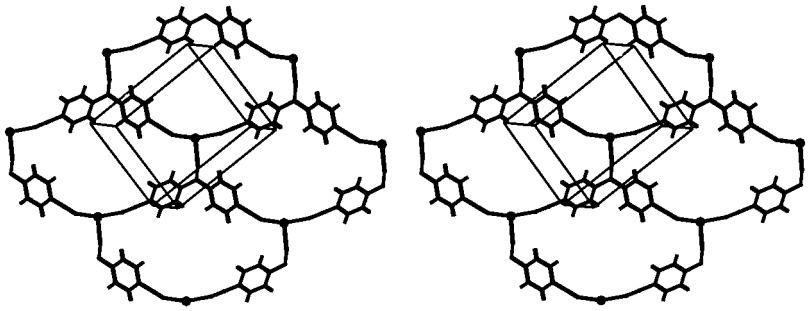

**Figure 3.** Stereoview of the graphitic sheet structure in complex **8**. Triflate ions incorporated in this structure are omitted for clarity. Large circles correspond to Ag sites.

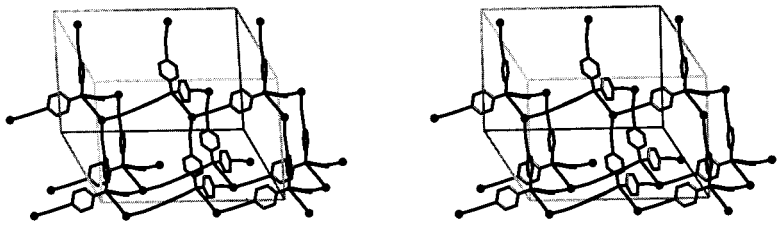

**Figure 4.** Stereoview of the diamond-like structure in complex **9**. The noncoordinating counterion tetrafluoroborates as well as incorporated solvent molecules are omitted for clarity. Large circles correspond to Ag sites.

overall structure is another honeycomb-type network structure with an average plane-to-plane distance of 3.74 Å. The Ag(I) ion is connected to two ligand nitrogen atoms, one ligand oxygen atom, and one triflate oxygen atom. The Ag−N distances are 2.218(3) and 2.226(3) Å while the Ag−O distances are 2.442(3) and 2.550(2) Å. Unlike complex **6** and **7**, no solvent molecules were found from the Fourier difference maps during the structure refinement.

**Diamond structure of [Ag·4·]$BF_4$·1.5$C_6H_6$ (9).** The crystal structure of **9** is illustrated in Figure 4. Each silver atom bonds to four ligand nitrogen atoms at Ag−N distances of 2.231(4), 2.253(5), 2.298(4), and 2.308(5) Å with N−Ag−N angles of 116.0(2), 115.6(2), 108.5(2), and 108.0(2)°. The silver atoms are in a distorted tetrahedral geometry. Unlike the triflate in the previous structures, the counterion tetrafluoroborate

(11) In all three cases of the complexes (**6**−**8**), the triflate counterion bonds to silver(I). This triflate−silver coordination is well-exemplified in other 14 crystal structures of the organosilver(I) triflate complexes reported by us and others.[2c−d,3a,c,4t,11b] A table of known organic silver triflate complexes is included in the Supporting Information. The triflate counterion always enters the coordination sphere of silver(I) if the crystallization solvent is an aromatic solvent such as benzene or toluene. Such "capping" effectively reduces the coordination number of silver(I) available for nitrogen-containing ligands to a maximum of three and inhibit it from forming the four-connected network. If the coordination number of the metal ion is four and the constituent ligand is tritopic, the (4,3) net is also possible as can be seen in ref 3d. (b) Hirsch, K. A.; Wilson, R. W.; Moore, J. S. *Inorg. Chem*. **1997**, *36*, 2960. (c) For the examples of bridging triflate ion in the silver(I) complexes, see refs 9, 11b, and 11d. (d) Buchholz, H. A.; Prakash, G. K. S.; Vaughan, J. F. S.; Bau, R.; Olah, G. A *Inorg. Chem*. **1996**, *35*, 4076.

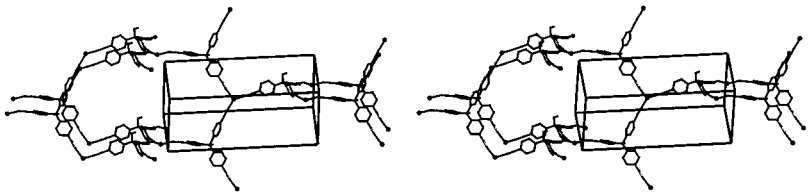

**Figure 5.** Stereoview of the $ThSi_2$-type structure of complex **10**. Solvent molecules as well as triflate ions incorporated in this structure are omitted for clarity. Large circles correspond to Ag sites.

is not coordinated to the Ag(I) ion. Each silver atom bonds to four terminal nitriles of the ligand **4** and each tetratopic ligand bonds to four silver atoms. This alternating arrangement of the ligands and the silver atoms forms a three-dimensional structure similar to the network found in diamond.

**$ThSi_2$ structure of $[Ag{\cdot}5{\cdot}CF_3SO_3]{\cdot}2C_6H_6$ (10).** The crystal structure of **10** is shown in Figure 5. The silver atom bonds to three ligand nitrogen atoms at Ag−N distances of 2.206(5), 2.249(4), and 2.428(5) Å, and one triflate oxygen atom at Ag−O distance of 2.362 Å. The hydroxyl group of the ligand does not bond to the Ag(I) ion. Instead, the hydroxyl group forms a hydrogen bond with a triflate oxygen atom at a distance of 2.0 Å.[12] Each silver atom bonds to three nitriles and each tritoptic ligand, three silver atoms. The resultant structure has a topology similar to a $ThSi_2$-type structure.[13]

## Discussion

As discussed in the Introduction, we and others have previously demonstrated that the use of symmetric, shape-persistent organic ligands, when combined with strong intermolecular directional bonding, often directs the resultant structures to analogues of well-known inorganic structures such as diamond and graphite. In such cases we find that the point group of the organic coordination solid and that of the corresponding inorganic structure type are often the same. In this paper, we have considered organic compounds of lowered symmetry in which the molecules still retain rigid orientations and fixed relative positions of the coordination bonding sites (in our cases the nitrogen or oxygen lone pairs). We have found that under these conditions lowering the symmetry of the molecule from $T_d$ to $C_{3v}$ and $D_{3h}$ to $C_{2v}$ does not alter the formation of the respective diamond and graphite-type structure. Furthermore, graphite-type frameworks continue to form even with the addition of pendant groups to the original rigid phenylacetylene framework. The introduction of a methoxy pendant group to central benzene in **1** leaves the resultant planar graphite structure rather unchanged.

**Chart 3**

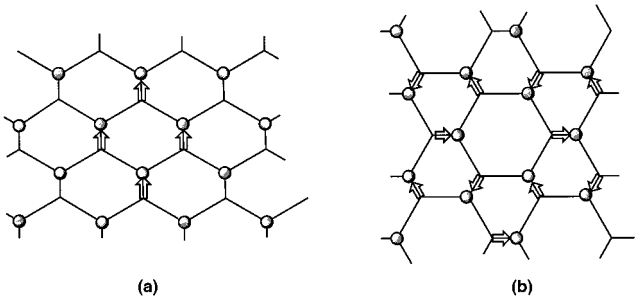


Unlike the more symmetric ligands of pseudo-$T_d$ and $D_{3h}$ symmetry, their $C_{3v}$ and $C_{2v}$ counterparts have permanent molecular dipole moments. To accentuate this dipole moment effect, we have functionalized the original backbones of $C_{2v}$ and $C_{3v}$ molecules with electron-donating or electron-withdrawing groups as can be seen in ligands **2**, **3**, and **5**. It is clear that the presence of such molecular dipole moments will have an effect on the formation of solid-state structure.[14] To understand the energetic relation between the individual molecular dipole moment and the crystal structure in our case we first consider in Chart 3 two paradigmatic graphite topologies.

In this chart the balls represent silver atoms and lines the $C_{2v}$ ligands while open arrows denote the molecular dipole moments. Such dipole moments are aligned along the 2-fold axes of the molecules. In Chart 3a, we illustrate the simplest possible graphite structure with one molecule per unit cell. The individual molecular dipole moments are therefore all pointing in the same direction. As a consequence, the single sheet has a permanent dipole moment. In contrast, Chart 3b illustrates the simplest sheet pattern in which there is no net dipole moment. This graphitic sheet structure has 3-fold axes perpendicular to the sheet. With such 3-fold symmetry, the molecular dipole moments cancel one another. If one considers only a single sheet of the structure by itself, simple electrostatic interactions suggest the pattern in Chart 3b without strong dipole−dipole interactions is lower in energy than the pattern in Chart 3a. However, this argument does not take into account the electrostatic interaction between neighboring sheets. It is possible to cancel the existing dipole

(12) See the examples of simultaneous interactions of hydrogen and coordination bonding in the self-assembled solids: (a) Dai, J.; Yamamoto, M.; Kuroda-Sowa, T.; Maekawa, M.; Suenaga, Y.; Munakata, M. *Inorg. Chem.* **1997**, 36, 2688. (b) Burrows, A. D.; Chang, C. W.; Chowdhry, M. M.; McDrady, J. E.; Mingos, D. M. P. *Chem. Soc. Rev.* **1995**, 329. (c) Burrows, A. D.; Mingos, D. M. P.; White, A. J. P.; Williams, D. J. *J. Chem. Soc., Chem. Commun.* **1996**, 97. (d) Burrows, A. D.; Mingos, D. M. P.; White, A. J. P.; Williams, D. J. *J. Chem. Soc., Dalton Trans.* **1996**, 149. (e) Munakata, M.; Wu, L. P.; Yamamoto, M.; Kuroda-Sowa, T.; Maekawa, M. *J. Am. Chem. Soc.* **1996**, *118*, 3117. (f) Nakasuji, K.; Tadokoro, M.; Toyoda, J.; Mitsumi, M.; Itoh, T.; Iijima, K. *Mol. Cryst. Liq. Cryst.* **1996**, *285*, 241. (g) Kosnic, E. J.; McClymont, L.; Hodder, R. A.; Squattrito, P. J. *Inorg. Chim. Acta* **1992**, *201*, 143. (h) Aakeröy, C. B.; Beatty, A. M. *J. Chem. Soc., Chem. Commun.* **1998**, 1067. (i) Aakeröy, C. B.; Beatty, A. M. Leinen, D. S. *J. Am. Chem. Soc.* **1998**, *120*, 7383.

(13) For the examples of possible three-dimensional, three-connected nets, see Wells, A. F. *Three-Dimensional Nets and Polyhedron*; Wiley: New York, 1977.

(14) The permanent dipole moment is an important factor leading to noncentrosymmetry in organic crystals. See: (a) Nicoud, J. F.; Twieg, R. J. In *Non-Linear Optical Properties of Organic Molecules and Crystals*; Chemla, D. S., Zyss, J., Eds.; Academic Press: New York, 1987; Vol. 1; p 253. (b) Meredith, G. R. In *Non-Linear Optical Properties of Organic and Polymeric Materials;* Williams, D. J., Ed.; ACS Symp. Ser. 233; American Chemical Society: Washington, DC, 1983; p 29.

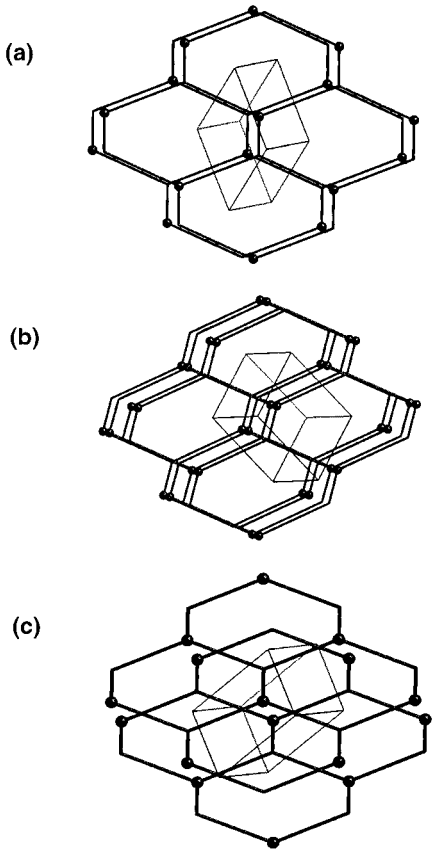


**Figure 6.** The stacking sequences for the three graphite-type nets of complexes **6**−**8**. The ligands are simplified as lines and silver atoms as balls for the sake of clarity. The coordinates for this figure are taken from the actual crystal structures. For complexes **6** and **7**, the centroids of the central benzene rings of the ligands are chosen as the center points while for complex **8** the carbonyl carbon is chosen as the center point. (a) (A·B·A·B) sequence found in complex **6**. (b) (A·A·B·B) sequence found in complex **7**. (c) (A·B·A·B) sequence found in complex **8**.

moment in pattern 3a through the introduction of a parallel sheet whose dipole moment is oriented in the opposite direction. Thus it is possible to create a crystal with no net dipole moment in pattern in Chart 3a as well as pattern in Chart 3b. In the three cases studied we find only pattern in Chart 3a. While they all have the same individual net topology, the stacking sequences of these nets are of two basic types (Figure 6). The stacking pattern for complex **6** is in an antiparallel fashion (A·B·A·B) so that the net dipole moment in a single sheet (A) cancels out the opposite dipole moment in the neighboring sheet (B) as can be seen in Figure 6a. A different stacking pattern is observed in complex **7** and **11**. In these cases the patterns are A·A·B·B sequences, as is illustrated in Figure 6b. Complex **8** shares the same pattern found in complex **6**.

That all four graphite-like layer structures adopt the same pattern of that in Chart 3a suggests the existence of a general energetic preference for this network type. It is well-known that the packing density is one of the most important factors in determining the stability of the crystal and that close-packed arrangements are lower in energy than loose-packed ones. In our case, the bond distances and bond angles between the silver ions and the ligands are fixed, and it is therefore possible to directly compare the densities of parts a and b of Chart

**Chart 4**

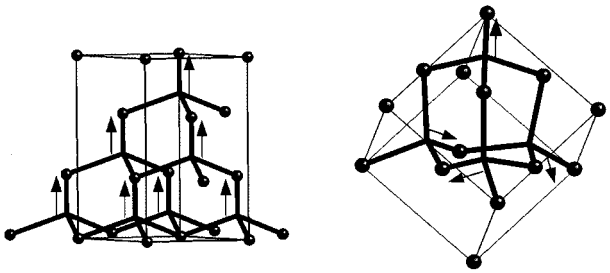

4a 4b

3. If one defines the 2D packing density $\rho$ as the number of the molecules per unit area, the ratio of the densities of the type in Chart 3b to type in Chart 3a ($\rho_b/\rho_a$) is $3(2x + 1)/(x + 2)^2$ (where $x$ ($0 < x < 1$) is the length of the short end of the ligand divided by that of the long end). An examination of this formula shows that the sheet pattern in Chart 3a is more densely packed than in Chart 3b for all values of $x$. The energetic preference for the network type in Chart 3a rather than in Chart 3b may therefore be due to the greater density possible with the Chart 3a type. However as net dipole moments are energetically costly the Chart 3a type sheets are stacked in a manner so as to cancel the dipole moments of adjacent sheets.

Similarly, permanent molecular dipole moments can be introduced into three-dimensional networks using $C_{3v}$ ligands. As in the previous examples of graphitic sheet structures, it is also possible to construct different types of diamond-like structures using the same $C_{3v}$ ligands.

Chart 4 illustrates two possibilities to form diamond-like structures from $C_{3v}$ ligand **9** (lines) and silver atoms (balls). The molecular dipole moments are indicated by arrows. The net pattern in Chart 4a is the simplest possible diamond-like structure and contains $C_3$ axes. Each molecular dipole moment is aligned along these axes. Thus, this diamond-type net has a net dipole moment. The simplest possible diamond network with no net dipole moment is illustrated in Chart 4b. In this structure some of the atom positions are shifted from their ideal geometry, resulting in a distorted version of the diamond net. Therefore, the molecular dipole moments in the unit cell point at the four corners of a hypothetical tetrahedron, thereby producing no net dipole moment. By comparing these two possible patterns, we can calculate the relative density as a function of $x$ where $x$ ($0 < x < 1$) is the ratio of the short end length of a $C_{3v}$ ligand to the long end length. The relative density of structure in Chart 4b to that in Chart 4a ($\rho_b/\rho_a$) is

$$\rho_b/\rho_a = \sqrt{2}/2(1 + 3x)(2t^2 + t + {}^1/_2)$$

where the packing density is defined as the number of the molecules per unit volume and

$$t = -\frac{1}{4}\left(\frac{16}{3x^2 + 2x - 5} + 1\right) - \frac{1}{4}\sqrt{\left[\left(\frac{16}{3x^2 + 2x - 5} + 1\right)^2 - 4\right]}$$

The function ($\rho_b/\rho_a$) is less than 1 in the entire range of $x$ ($0 < x < 1$), demonstrating that pattern in Chart 4a is

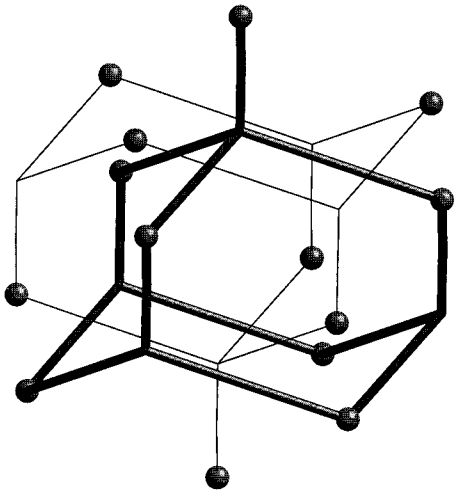

**Figure 7.** A portion of the double-diamond structure of complex **9**. Two independent, adamantane-like nets interpenetrate each other to form the double-diamond structure of **9**.

more dense-packing than pattern in Chart 4b. Though pattern in Chart 4a is favored by the density of packing, pattern in Chart 4b would be lower in energy if one considers only the electrostatic interaction among neighboring electric dipole moments. However, similar to the previously mentioned graphitic structures, an interpenetration of two identical nets in opposite directions will result in cancellation of the permanent dipole moment in each single net. Figure 7 illustrates two independent, interpenetrating diamond nets observed in complex **9**. In this structure, a 2-fold interpenetration occurs with respect to the inversion center. Therefore, while a single diamond net has a permanent dipole moment, two interpenetrating nets with opposite permanent moments result in zero net dipole moment. As in the cases of the graphitic sheets, experimentally, we only find the more dense-packing network. Also just as in the graphite case we find that two networks with exactly opposite dipole moments are placed adjacent to each other thus canceling out their dipole moments. However, because the latter systems are composed of three-dimensional networks, these adjacent nets must interpenetrate one another to achieve this cancellation.

Finally, it can be noted that the overall structure of complex **9** is an analogue of the double-diamond structure, a structure well-known in the literature of mesoporous solids.[15,16] The double-diamond structure is found in amphiphilic systems such as lipids, block copolymers, and liquid crystals which contain two chemically distinct components for which an interface is formed.[17,18] In the case of the crystal at hand the two components in the crystal are the well-crystallized host network and the less well-crystallized solution molecules found at the surface of the host network.

**Acknowledgment.** The authors are grateful to Dr. Jeffrey Kampf of the University of Michigan and Dr. Emil Lobkovsky of Cornell University for collecting the single-crystal X-ray data sets. This research was supported by National Science Foundation (DMR-9812351).

**Supporting Information Available:** Tables of crystal refinement data, positional parameters, anisotropic displacement parameters, bond lengths and angles together with observed and calculated structure factors, as well as powder diffraction data. This material is available free of charge via the Internet at http://pubs.acs.org.

CM981153C

(15) For the examples of double-diamond structures, see: (a) Bragg, L.; Claringbull, G. F.; Taylor, W. H. *Crystal structure of Minerals;* Cornell University Press: New York, 1965. (b) Wells, A. F. *Structural Inorganic Chemistry*, 4th ed.; Clarendon Press: Oxford, U.K., 1975; p 102. (c) Kim, K.-W.; Kanatzidis, M. G. *J. Am. Chem. Soc.* **1992**, *114*, 4878. (d) Sofen, S. R.; Cooper, S. R.; Raymond, K. N. *Inorg. Chem.* **1979**, *18*, 1611. (e) Vossmeyer, T.; Reck, G.; Katsikas, L.; Haupt, E. T. K.; Schulz, B.; Weller, H. *Science* **1995**, *267*, 1476. (f) Ermer, O. *Helv. Chim. Acta* **1991**, *74*, 825. (g) Hoskins, B. F.; Robson, R. *J. Am. Chem. Soc.* **1990**, *112*, 1546. (h) Thomas, E. L.; Alward, D. B.; Kinning, D. J.; Martin, D. C.; Handlin, D. L., Jr.; Fetters, L. J. *Macromolecules*, **1986**, *19*, 2197. (i) Matsushita, Y.; Tamura, M.; Noda, I. *Macromolecules*, **1994**, *27*, 3680. (j) Longley, W.; McIntosh, T. J. *Nature* **1983**, *303*, 612.

(16) For examples of higher degree of interpenetration such as 3-fold,[16a−c] 4-fold,[16d,e] 5-fold,[16f] 6-fold,[16g] 7-fold,[16h,i] 8-fold,[16j] and 9-fold,[16k] see: (a) Ermer, O.; Eling, A. *Angew. Chem., Int. Ed. Engl.* **1988**, *27*, 829. (b) Michaelides, A.; Kiritsis, V.; Skoulika, S.; Aubry, A. *Angew. Chem., Int. Ed. Engl.* **1993**, *32*, 1495. (c) Reddy, D. S.; Craig, D. C.; Desiraju, G. R. *J. Am. Chem. Soc.* **1996**, *118*, 4090. (d) Reference 4h. (e) Reference 4l. (f) Ermer, O. *J. Am. Chem. Soc.* **1988**, *110*, 3747. (g) Konoshita, Y.; Matsubara, I.; Higuchi, T.; Saito, Y. *Bull. Chem. Soc. Jpn.* **1959**, *32*, 1221. (h) Ermer, O. *Adv. Mater.* **1991**, *3*, 608. (i) Sinzger, K.; Hünig, S.; Jopp, M.; Bauer, D.; Bietsch, W.; von Shütz, J. U.; Wolf, H. C.; Kremer, R. K.; Metzenthin, T.; Bau, R.; Khan, S. I.; Lindbaum, A.; Lengauer, C. L.; Tillmanns, E. *J. Am. Chem. Soc.* **1993**, *115*, 7696. (j) Reference 12a. (k) Reference 4t.

(17) The interface of double-diamond may be compared with a mathematical model for tetrahedral minimal surface by Schultz. See: Schwarz, H. A. *Gesammelte Mathematische Abhandlung*; Springer: Berlin, 1890; Vol 1.

(18) Anderson, D. M.; Davis, H. T.; Scriven, L. E.; Nitsche, J. C. C. *Adv. Chem. Phys.* **1990**, *77*, 337. (b) Charvolin, J.; Sadoc, J. F. *J. Phys.* **1987**, *48*, 1559. (c) Andersson, S.; Hyde, S. T.; Schnering, H. G. v. *Zeit. Kristallogr.* **1984**, *168*, 1.